The influence of a bulk twist on the surface memorization in the liquid crystal HOBA

M. Petrov; L. Tsonev

PLEASE SCROLL DOWN FOR ARTICLE

Taylor & Francis
Taylor & Francis Group

The influence of a bulk twist on the surface memorization in the liquid crystal HOBA

M. PETROV and L. TSONEV*

Institute of Solid State Physics, Bulgarian Academy of Sciences,
72 Tzarigradsko Chaussee blvd., 1784 Sofia, Bulgaria

The surface-induced memorization of a smectic C liquid crystal texture in the temperature range of the nematic phase of 4-*n*-heptyloxybenzoic acid oriented by obliquely evaporated SiO on ITO was removed by imposing a bulk twist (Prevention of surface memorization was not observed when we used a simple ITO coating as the orienting surface.) A twist angle value ($\Omega_c \approx 70°$) above which the surface memorization is prevented was found. Using microtextural polarization analysis of the smectic C texture, a qualitative explanation of the phenomenon is suggested. The conditions for preventing the surface memorization were deduced in terms of the balance between the surface and bulk torques. These conditions provide surface anchoring breaking, so removing the surface memory effect.

1. Introduction

The surface memory effect (SME) is a surface phenomenon resulting from the complex character of the interface 'liquid crystal–solid surface'. Two different kinds of SME can be investigated: (i) memorization of an oriented nematic (N) texture on filling a liquid crystal cell (LCC) in the nematic temperature range due to the 'flow alignment effect' [1] and (ii) memorization of a smectic (A or C type) texture in the temperature range of the nematic state [2, 3]. In the smectic case, the main role in the memorization is played by the thermal energy of normal physical adsorption which is about $80 \, kJ \, mol^{-1}$. Therefore the SME mechanism cannot be restricted to the consideration of a 'liquid crystal–solid surface' interface as is usually done in the case of elastic surface anchoring described by the surface energy of Rapini Papoular [4], as well as of the Berreman model [5] of the elastic adaptation of the LC to the orienting grooved surface. The problem of physical-chemical forces acting in the interface domains, such as anisotropic long range van der Waals type forces or short range steric forces is still open. Recently [3, 6–8] we investigated the surface memorization of smectic C textures in the nematic temperature range for some homologues of the 4-*n*-alkyloxy-benzoic acids, namely $n = 7$ (HOBA), $n = 8$ (OOBA) and $n = 9$ (NOBA), showing that in these materials the usual physical adsorption and the monolayer formed due to this adsorption at the 'liquid crystal–solid surface' interface cannot explain the experimental results. We have found that the SME erasure activation energy Q

measured in the frame of the 'rotational diffusion model' [9]—where Q was evaluated from the expression for the temperature dependence of the erasure time t_{er} in the static erasure process $t_{er} = t_o \exp(Q/k_B T)$, where k_B is the Boltzmann constant and t_o is an extrapolation constant (2.1 eV [9] for octylcyanobiphenyl oriented by polyimide and 4 eV for 4-*n*-alkyloxybenzoic acids oriented by SiO oblique evaporation [3])—is 2–4 times higher than the physical adsorption energy Q_{ads}, which is usually about 1 eV. The difference $Q - Q_{ads}$ was also investigated in other phenomena such as induced surface order polarization [6], double electric layers [6, 7] and mechanical effects due to the surface topography [5, 8]. In correspondence with these ideas, we presented the total activation energy Q [7] as a sum of different components: $Q = Q_{ads} + Q_{el} + Q_{mech} + \delta Q$, meaning adsorption ($Q_{ads}$), electric (dielectric) (Q_{el}), mechanical ($Q_{mech} + \delta Q$) energy, respectively. The component δQ represents mechanical energy connected only with the surface topography [5]. By varying the cell wall coatings and using counteractive clearing agents against the memorization processes (e.g. an external electric field [7]) we estimated the various components of Q.

In this paper, we want to throw more light on the components $Q_{mech} + \delta Q$ in the erasure activation energy. It is well known [10] that the surface and the bulk states of the LC are coupled and modified by various external influences. We found experimentally that in a normal cell filled with HOBA and with SiO/ITO/glass walls, which in the untwisted state gives a normal SME, loses its memorization ability completely after a $\pi/2$ twist (bulk twist SME prevention). We studied the nature

*Author for correspondence; e-mail: lyubo@issp.bas.bg

and the value of the twist angle making the memorization impossible, an effect which is equivalent to the erasure of the memorized texure by the thermal factor $k_B T$ for example.

In order to understand the role of the imposed bulk twist on the SME, we recall some macroscopic properties of the N phase of these 4-*n*-alkyloxybenzoic acids which involve hydrogen-bonded molecules. The nematic phase of these acids which display both N and SmC phases (e.g. HOBA in our case) has been investigated by different methods such as microtextural polarization analysis, electro-optic depolarizing Rayleigh light scattering [11], DSC, impedance [12] and IR spectroscopy [13]; it was found that in the middle of the nematic temperature interval a specific temperature T^* exists below which the macroscopic properties (e.g. texture) sharply change. Various surface orientations of the N phase were used [14–17] in order to understand the nature of this temperature. Up to now it is known that this temperature always exists, but by using suitable boundary conditions (surface coatings) it can be visualized in a very pronounced manner [14, 16] (at dielectric coatings: SiO/glass) or depressed [6] (at conducting coatings: ITO/glass, SiO/ITO/glass). Actually it was found that a pronounced texture transition can be observed (e.g. for HOBA) at SiO/glass cell walls [16], as this transition was accompanied by a spontaneous twist at a temperature $T^\varphi > T^*$. In this case we did not observe SME [6]. On the contrary, at conducting coatings such as ITO/glass, SiO/ITO/glass, one cannot observe a texture transition at T^* [6], but a strong SME exists. We have detected that static erasure—by simple annealing—of the memorized texture is possible only above T^*, where the nematic behaviour is like that of conventional nematics (e.g. MBBA), meaning that below T^* one cannot erase the memorized texture. The quasi-smectic layer structure due to cybotactic groups [18] below T^* was assumed to be responsible for the strong SME [3].

By an imposed bulk twist it was found that for the dielectric coating SiO/glass the temperature T^* [14] and the spontaneous twist temperature $T^\varphi > T^*$ [16] shift a few degrees downwards with respect to the case where a planar homogeneous orientation is obtained using the same dielectric boundary conditions. In the conducting case, T^* and a spontaneous twist are not observed by texture transition. The spontaneous twist for dielectric coatings was explained by order electric polarization **P** parallel to the SiO/glass surface (for details see [16, 17]) or by cybotactic chiralization [19].

A spontaneous twist could exist in the frame of cybotactic groups due to possible chiralization provided by variation of the hydrogen bonds—oligomerization (see for details [19]), which cannot develop macroscopically in the conducting case. Thus in the conducting

cases of ITO/glass and SiO/ITO/glass where spontaneous twist does not exist, one can impose purely bulk twist by strong surface anchoring, so providing SME prevention [3]. The SME as related to the memorization of smectic A or C type textures can really be realized only in nematics with short range smectic A or C order (meaning above SmA or SmC phases), where cybotactic groups or quasi-layering exists [3, 4]. In this sense, the SME regarded as 'flow alignment' [1] exists only in conventional nematics, but the SME involving memorization of smectic textures exists only in nematics with short range smectic order due to cybotactic groups.

Note that in nematics with short range smectic C order (e.g. 4-*n*-heptyloxyazoxybenzene, HOAB) a temperature like T^* does not exist, due to the absence of hydrogen bonds in the molecules, and this nematic phase resembles only the N_2 subphase of HOBA. The surface memorization in this case can be erased only in the isotropic phase, while in HOBA the memorization can be erased also in the N_1 subphase (i.e. classical nematic phase) where cybotactic group action is negligible.

2. Experimental results

There is a significant difference between the bulk twist and the thermal activity $k_B T$ [3] or the electric field [7] when used as external influences against the SME. The twist action is applied before growth of the smectic C phase and counteracts the memorization, while the thermal activity and electric fields are applied in the nematic temperature range after memorization of a smectic C texture has occurred. In this sense the bulk twist prevents memorization, while the thermal activity and external electric fields erase existing memorization.

To study the SME we chose HOBA for which measurements indicate weaker memorization and thus easier erasure (e.g. by thermal activity or electric fields), showing therefore a higher sensitivity with respect to additional influences.

The phase transition temperatures (°C) of HOBA are:

$$Cr \xleftrightarrow{92} SmC \xleftrightarrow{98} N \xleftrightarrow{146} I$$
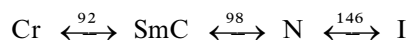
We prepared two types of LC cell (LCC) according to the cell wall coatings used: ITO layers on glass and obliquely evaporated SiO on ITO on glass, since the SME is realized only in LCC with conductive coatings, but not in LCCs with purely dielectric plates [6]. The cell thickness d was varied between 5 and 250 μm using Mylar spacers. The SiO layers were obliquely evaporated at an angle α (between the surface normal and the evaporation direction) of 60° and with a layer thickness δ of 45 nm. Under such evaporation conditions [20, 21], the LC system displays monostable unidirectional alignment characterized by a director $\mathbf{n}_o$ perpendicular to the

evaporation plane. The monostable unidirectional alignment was a necessary element in the geometry of our experiment.

In the cells with ITO/glass walls ($Q = 2$ eV) at various thickness values (5–250 μm) and twist angles (0–$\pi/2$), we always observed the SME. Real interest was provoked by the cells with SiO/ITO/glass walls: the memorization without twist was normal ($Q = 2.4$ eV); at $\pi/2$ twist, however, the surface memory effect was totally absent. Consequently, we expected to find a twist value (Q_c) between 0 and $\pi/2$ at which prevention of the SME begins. The physical sense of this point will be discussed.

We prepared our SiO/ITO/glass cells by capillary filling in the isotropic phase. Dealing with twist, we ensured that the LC system and the polarized light of wavelength λ were in the Maugin regime, so that the linearly polarized light follows the nematic director between the front and exit glass plates. We checked the twist cell using a microscope with crossed polarizers (polarizer P and analyser A, P$\perp$A). In such a geometry, with a $\pi/2$ twist, the nematic texture is bright between crossed and black between parallel polarizers. We realized the variation of the twist angle between 0 and $\pi/2$ in two ways.

(1) The cell plates were first mutually rotated until their 'easy' axes made the desired angle Ω; then the cell was heated up above $T_{N\text{-}I}$ and filled up with the liquid crystal substance by capillary forces.

(2) The cell with parallel oriented 'easy' axes of the plates was filled with the liquid crystal substance in the isotropic phase and then the upper plate was rotated with respect to the lower plate (keeping the chosen gap constant) until their 'easy' axes made the desired angle.

Each eventual correction of the angle Ω in one and the same LCC was made only in the isotropic phase of the substance studied.

Using various twisted cells with Ω between 0 and $\pi/2$ we looked for the evolution of recording and erasure of the smectic C texture in the nematic temperature range for HOBA in SiO/ITO/glass cells. The polarization microtextural analysis showed that in the region $0 < \Omega < 69°$ the SME is present with a definite strength $\tau \neq 0$ where $\tau = t_{er}/t_{rec}$ and t_{rec} and t_{er} are, respectively, the recording and erasure times for a given texture [3]. In the region $71° < \Omega < 90°$ there is no memorized smectic C texture. Exactly at $\Omega = 70°$, the memorized smectic texture transformed, after the phase transition, into a nematic texture, typical for the chosen geometry, with very weak contrast which was erased immediately, implying almost zero strength, $\tau \approx 0$. Therefore we consider $\Omega_c = 70°$ as the twist preventing the SME (figure 1).
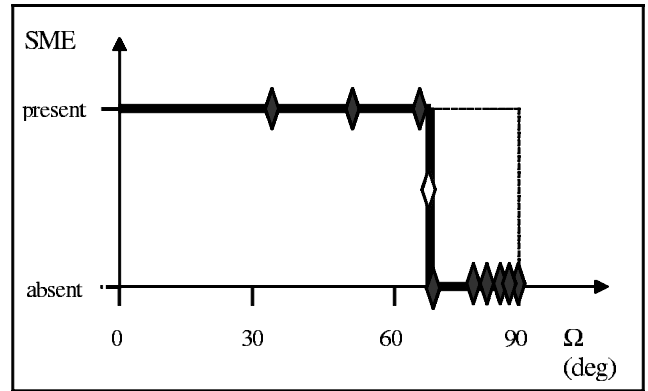

Figure 1. Presence or absence of surface memorization in HOBA as function of the cell twist angle.

Figures 2, 3, 4 and 5 illustrate the SME observations for HOBA filled SiO/ITO/glass cells with $d = 20$ μm for $\Omega = 36°$ (figure 2), 70° (figure 3), 71° (figure 4) and 90° (figure 5). The experimental conditions for taking the photographs in figures 2(a)–5(a) were as follows: $t_{rec} = 15$ min and $T_{rec} = 96°C$ (in the smectic temperature range). In figures 2(b)–5(b), the phase transition front is shown crossing the cell at the transition temperature $T_{SmC \to N} = 98°C$. The photographs in figures 2(c)–5(c) were taken at 112°C, i.e. above the transition temperature, in the nematic phase, without retardation, i.e. $t_{er} = 0$. We chose this temperature (112°C) to be a few degrees below T^*_{HOBA} equal to 117°C in the planar orientation (see [3]) and 114.5°C at $\Omega = \pi/2$ in the interval of the N_2 phase. Therefore the thermal erasure action was avoided (see [3]) and only twist action was demonstrated. Full SME prevention is demonstrated in figure 4(c) for a twist angle only one degree above the critical value. The twist angle was measured with an accuracy of $\pm 1°$.

Next we carried out a similar investigation on the critical twist as a function of the cell thickness. The conclusion obtained was that $\Omega_c \approx \text{const}(d)$ in the interval $5 < d < 250$ μm. This fact indicates that actually the bulk action dominates over the surface in the studied phenomena. We measured also the erasure activation energy Q and the memory strength τ at different twists. The result is:

$$Q = \text{const}(\Omega) = 2.4 \text{ eV}$$

and

$$\tau = \text{const}(\Omega) \ll 1 \text{ (very weak SME) for } 0° < \Omega < 70°.$$

Finally, let us stress that twist never prevents the surface memory effect for HOBA in ITO/glass cells. Therefore the role of the obliquely evaporated SiO is very important for depressing the process of surface memorization.
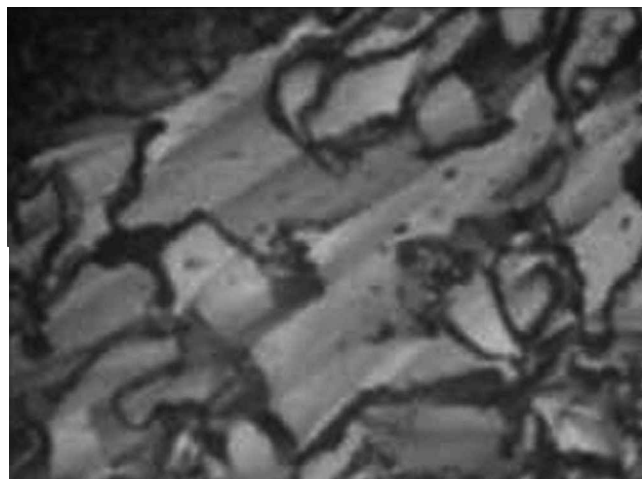
(a)
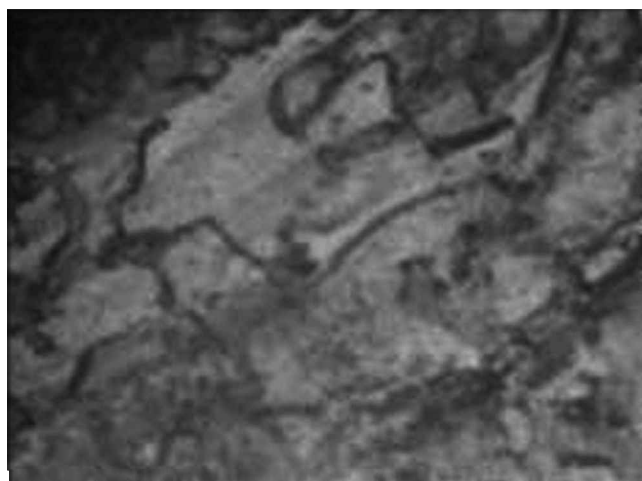
(b)

(c)

Figure 2.   Surface memorization status in an HOBA cell with SiO/ITO coated walls for twist angle $\Omega = 36°$. (a) Smectic phase; (b) transition smectic $\rightarrow$ nematic state; (c) nematic phase.
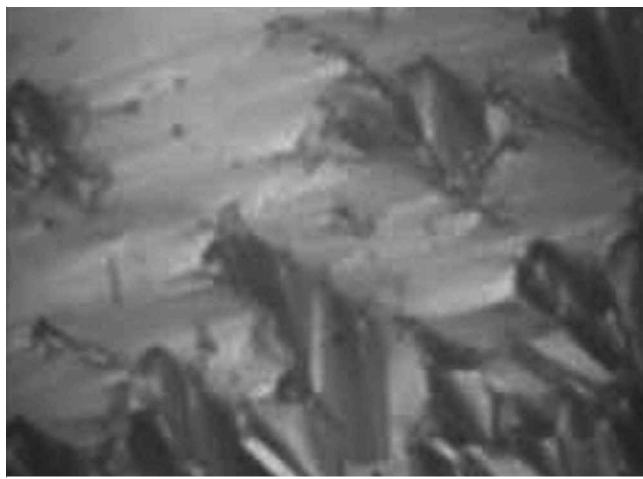
(a)

(b)

(c)

Figure 3.   Same as figure 2, but for $\Omega = 70°$.

(*a*)

(*b*)

(*c*)

Figure 4.   Same as figure 2, but for $\Omega = 71°$.

(*a*)

(*b*)

(*c*)

Figure 5.   Same as figure 2, but for $\Omega = 90°$.

3. Discussion
3.1. *Preliminary remarks*

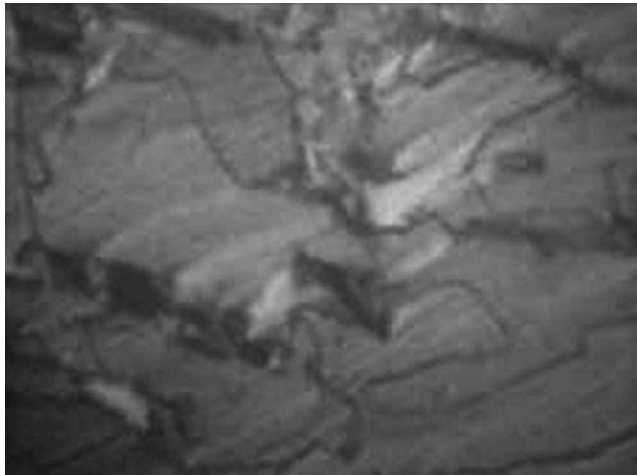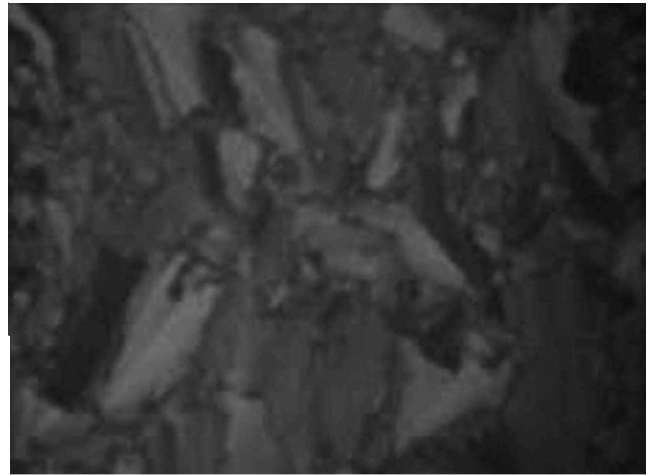Before starting the discussion we should recall one important fact [6]. The SME for HOBA was observed in cells with conducting wall coatings (ITO/glass or SiO/ITO/glass), but never in cells with dielectric walls (clean glass or SiO/glass). Using the term 'conducting', however, we must be more precise due to the difference in conductivity values for ITO/glass and SiO/ITO/glass systems. For the specific conductivity, measurements give: $\rho(\text{ITO}):\rho(\text{SiO}/\text{ITO}):\rho(\text{SiO}/\text{glass}) = 10:10^{3}:10^{a}$, where $a > 8$. Therefore the SiO/ITO/glass system (deposition angle $\alpha = 60°$, layer thickness $\delta = 45$ nm for SiO) represents more a conductive than a dielectric case. In the present experiments using conducting coating ITO/glass, we found that the SME can never be prevented or removed by twist action. For a dielectric case (pure glass or SiO/glass) memorization fails in principle [6], without any connection with cell twisting. Using the quantitative results for this dielectric orienting surface case, an explanation for the absence of SME was presented in [6]. In the dielectric SiO/glass case, a spontaneous twist can be realized in nematic state above T^* (see §1). This twist is related to the coupling between the surface (probably order) polarization $\mathbf{P}_o$ and associated horizontal depolarizing field $\mathbf{E}$, since the twist disappears in the presence of conducting ITO or SiO/ITO coatings [16, 17]. Thus the surface order polarization in the dielectric case provides spontaneous surface twist and depresses the SME. We did not observe spontaneous surface twist in ITO/glass and SiO/ITO/glass cases.

SME prevention by imposed twist was observed only in the SiO/ITO/glass case, but not in the ITO/glass case. Consequently, the imposed bulk counteraction (twist) created by the elastic bulk effect modifies the memorizing property of the surface (SiO/ITO/glass system), preventing in such a way the SME over some imposed twist angle Ω_c.

Let us now discuss the mechanism of the SME weakening when the SiO layer obliquely evaporated on the typical conducting ITO layer is attacked by a bulk twist. One has to be very careful to exclude other SME depressing bulk factors from the experimental conditions. We shall recall here the mechanical and anchoring abilities of a SiO layer obliquely evaporated on ITO/ glass (SiO/ITO/glass case), comparing them with the ITO/glass case, keeping other experimental conditions identical. The experimental geometry of a SiO/ITO/glass plate is presented in figure 6.

It is well known [20, 21] that for a fixed thickness δ of the SiO layer (usually between 20 and 50 nm) variation of the evaporation angle α gives rise to three basic LCC orientations: (i) for $\alpha < 60°$—monostable uniform
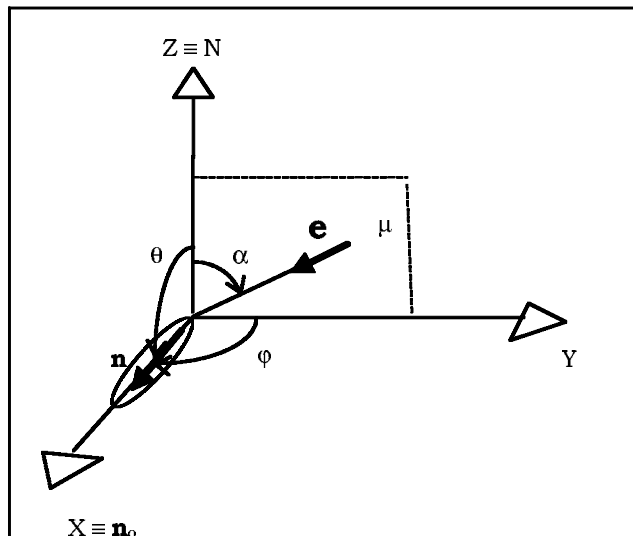
Figure 6. Scheme of the oblique SiO deposition. **e**, α, μ—direction, angle and plane of evaporation, respectively. **n**, θ, φ—'easy' direction, polar and azimuthal angle of the liquid crystal molecules, respectively.

orientation of the molecules in the direction perpendicular to the evaporation plane, polar angle $\theta = \pi/2$, azimuthal angle $\varphi = \pi/2$; (ii) for $60° < \alpha < 75°$—bistable orientation, two easy axes $\mathbf{n}'$, $\mathbf{n}''$ are generated for minimization of the surface energy with angles φ, $-\varphi$, θ; (iii) $\alpha > 75°$—the monostable uniform orientation of **n** is tilted but lying in the evaporation plane μ, i.e. $\varphi = 0$, $\theta \neq 0$. Certainly each of these three evaporation geometry conditions will have different effects in the prevention or enhancement of the SME, but we consider here only the first case ($\alpha = 60°$).

We always prepared our samples at $\Omega = 0$ in a symmetrical way (figure 7) so that the evaporation directions

Figure 7. Scheme of the untwisted cell, i.e. for $\Omega = 0°$; d = cell thickness.

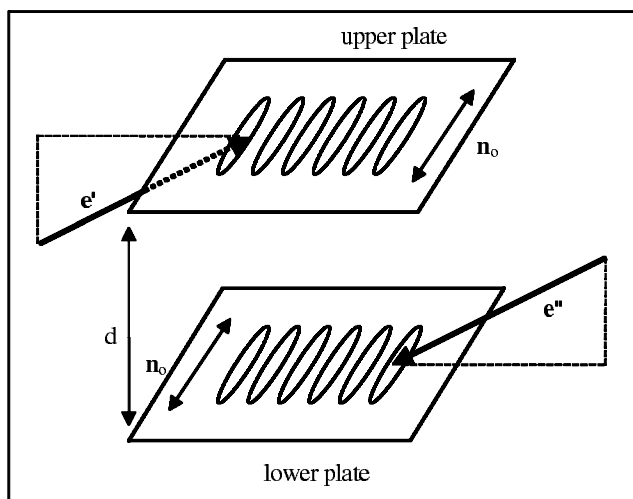of the two cell walls are mutually parallel. With the symmetric LCC preparation we avoided (although we know that **n** is not tilted, $\theta = \pi/2$) any complex elastic deformation—combination of bend, twist and splay. In this manner of preparation we expected the imposed twist $0 < \Omega < \pi/2$ by rotation of one of the plates (the upper one) with respect to the fixed position of the other to be pure twist. In our case for $\theta = \pi/2$ (meaning that **n** lies close to the plate surface) this requirement is easily fulfilled. Therefore by the parameters α and δ of the evaporation process, the initial values of the polar coordinates φ_o and θ_o of the director $\mathbf{n_o}$ are fixed. Each external excitation (mechanical, electric, magnetic) obviously deviates the $\mathbf{n_o}$ position to the state which minimizes the surface energy, thus inducing a new director position $\mathbf{n_s}$ with new angular coordinates $\theta \neq \theta_o$, $\varphi \neq \varphi_o$.

One very important detail in the orienting role of the SiO evaporated layer is its microstructure, providing the anisotropy of the surface. By analogy with other cases of oblique evaporation of different materials on various substrates [22, 23] and using the electron diffraction method (scanning electron microscopy) it has been demonstrated [24] that the evaporated SiO layer has grown as an aggregate of microcolumns tilted in the evaporation plane (tilt angle α_c). For the evaporation at $\alpha \leqslant 60°$, it was indicated that the microcolumnar structure is finer and a clustering of columns perpendicular to evaporation plane (direction x) is observed. The columnar angle α_c can be considered to be more or less independent of α and has a value of $22 \pm 4°$. Therefore two different structural properties are present in obliquely evaporated SiO layers: one kind of anisotropy is due to the columnar growth in the zy plane and the second kind is due to the clustering of columns perpendicular to this plane (i.e. in the x direction), which is our case.

3.2. *Interpretation*

In order to indicate some fundamental properties of the twist, we present in figure 8 the case $\Omega = \pi/2$. x and y are easy directions of **n** ($\mathbf{n_o}$) which are perpendicular to the evaporation planes zy and zx, respectively. A possible scheme showing the molecular positions in this case of a twisted liquid crystal is presented in the figure. From investigations using crossed and parallel polarizers, it follows that at strong anchoring the molecules in contact with the upper and lower cell walls are oriented in the x and y easy directions. The twist deformation begins at the plate surface and penetrates the volume. We are interested in the molecular position in the middle of the LCC. Some of the possible molecular positions are presented in figures 8(a) and 8(b). They are connected with the direction of the applied torques with respect to
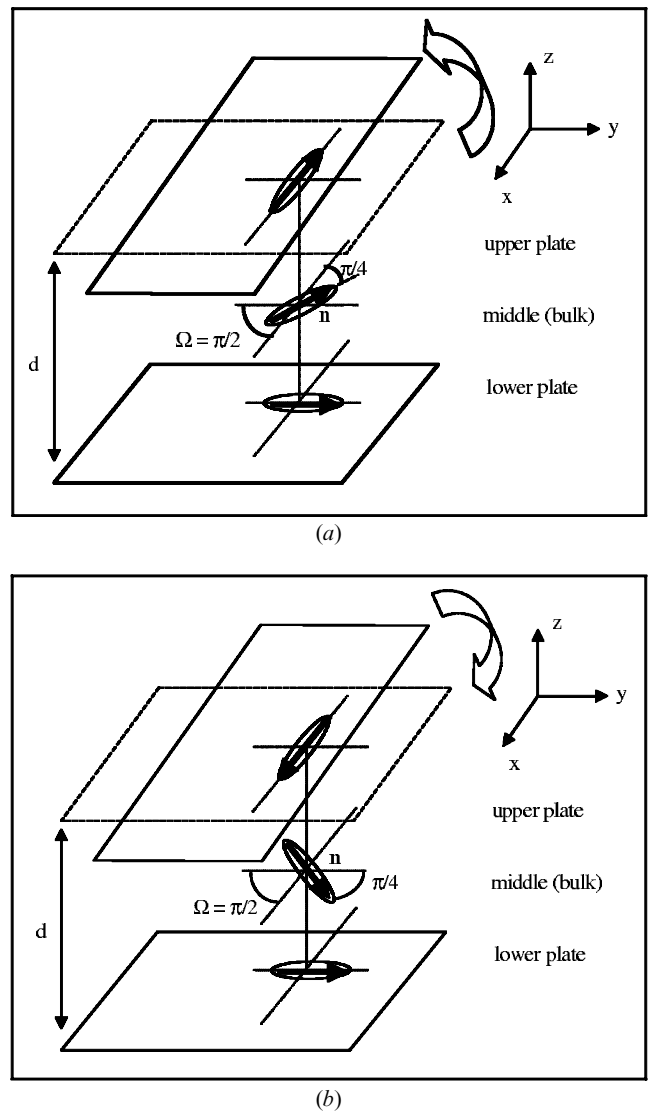
Figure 8. Scheme of the twisted cell for $\Omega = 90°$; (a) and (b)— two possible rotation directions.

n (for twist deformation). It is seen that with torques with opposite directions eventually created from the upper and lower plates, the configuration of the molecules in the middle region will be such that **n** will make an angle $\pm \pi/4$ with the easy directions x, y.

For the case ($\Omega = \pi/2$) the smectic layer at the surface grows vertically or obliquely to the boundary. It follows from known fact [25] that the twist texture with the layer parallel to the substrate (xOy plane) is not favourable since the twist is a deformation which requires less energy ($K_{22}\Omega^2/d$) with respect to the splay and bend distortion energy ($K_{22} < K_{11} < K_{33}$). Thus parallel to the surface, layer orientation can be realized without local distortion of the uniform molecule orientation, which is not our case. It is seen from the photographs in figures 2(a)–5(a) that the elongated, single local monodomains

(SLM) formed are separated by π inversion walls and their long axes are oriented in different directions with respect to the 'easy' axes.

With SmC growing in the presence of bulk twist excitation, the orientation of the long axes of the SLM and the surface defects (π-inversion walls) reflect the growth of the smectic layers on cooling.

When the bulk twist, that is $K_{22}/d(\Omega^2)$, increases, the disorder of the surface orientation of the SLM grows. In figure 5(a) ($\Omega = \pi/2$) the SLMs are disordered with respect to the case when $\mathbf{n} \equiv \mathbf{n}_o$ and $\Omega = 0$. In the last case the surface dominates and the SLMs are oriented in such way that $\mathbf{n}$ follows the 'easy' direction ($\perp$ to the evaporation plane) and the layers are vertical to the xy surface and make some angle with the 'easy' direction (usually the angle is equal to $\pi/4$ which is temperature independent of the tilt of $\mathbf{n}$ for this substance with respect to the smectic C layer) (see figures 9 and 10). Thus at $\Omega = 36°$ and $\Omega < 70°$, as well as at $\Omega = 0$, the SLM are oriented nearly at $\pm\pi/4$ with respect to the 'easy' direction, which is the direction of the smectic layers. In figure 10 the SLM are presented as elongated ellipses with long axes ($\mathbf{l}$) which coincide with the orientation of the molecular layers $\mathbf{s}$ forming the SLM.

The above analysis can be illustrated by the photographs in figures 2(a)–5(a). As seen in figure 2(a) where the twist is weak ($\Omega = 36°$) and more closely to the case $\Omega = 0$ (figure 9) where the 'easy' axes of the upper and the lower plates are parallel, the long axes of the SLM make the angle $\pm\pi/4$ with the two 'easy' axes.

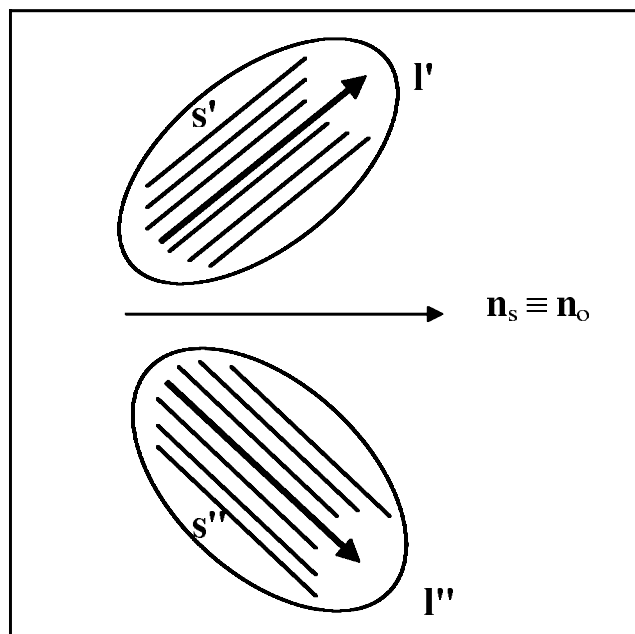Figure 9. Same as figure 2, but for $\Omega = 0°$; memorized texture in the smectic phase.

Figure 10. Scheme of local monodomains below the critical twist angle $\Omega < \Omega_c$. $\mathbf{s}', \mathbf{s}''$—layer directions; $\mathbf{l}', \mathbf{l}''$—long axes; $\mathbf{n}_o$—'easy' direction, $\mathbf{n}_s$—surface director.

The evolution of the SmC texture with increasing twist deformation Ω demonstrates that at $\Omega = 70°$, $71°$ and $\pi/2$ (figures 3(a), 4(a) and 5(a), respectively), the orientation of the long axes of the SLM is $\perp$ or $\parallel$ to the $\mathbf{n}_o$ direction (see figure 11). This implies that starting with $\Omega = 70°$, the bulk dominates over the surface and the texture (meaning coordination of $\mathbf{n}$ with the layer orientation $\mathbf{s}$) is independent of the surface anchoring and especially of its azimuthal component $f_s(\varphi)$. In this case the bulk torque dominates over the surface torque. On the contrary for $0 < \Omega < 36°$, the magnitude of the bulk twist is not high enough and the surface azimuthal anchoring dominates, thus orienting the SLM according to the surface conditions expressed by the easy axis and the elastic anchoring strength. That is why $\Omega_c = 71°$ is the twist value at which the bulk twist torque is sufficient to surpass the surface torque.

Let us analyse the phenomenon on the basis of the surface anisotropy and the corresponding balance of surface and bulk forces. Two possible alignment forces act here simultaneously—a physical–chemical one due to van der Waals forces, and the topographical elastic adjustment, providing both the anisotropy and the orienting properties of the surface; consequently two mechanisms for creating the anisotropy of the SiO surface exist.

The first (physical–chemical) mechanism is expressed in the adsorption of the liquid crystal molecules of the alkyloxybenzoic acid (characterized by dimer ring and H bonds) directly on the SiO surface, thus forming
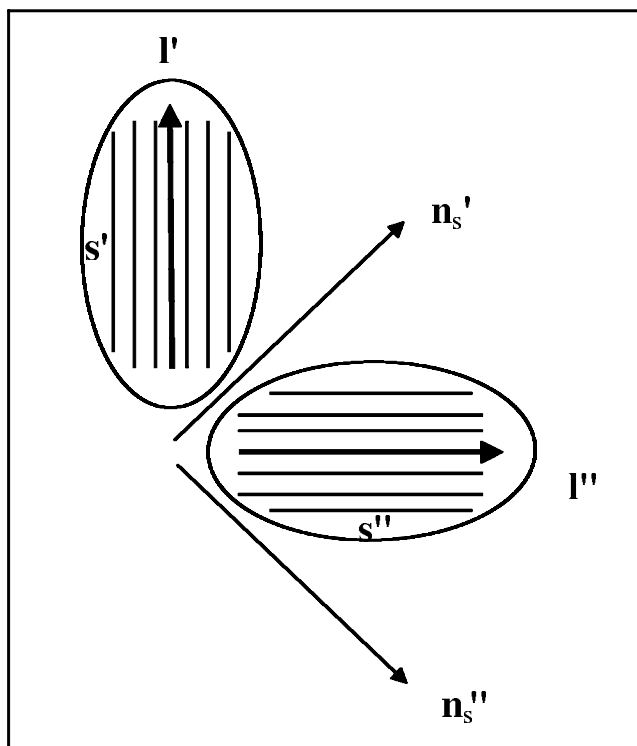
Figure 11. Scheme of local monodomains above the critical twist angle $\Omega > \Omega_c$; $\mathbf{n}'_s$, $\mathbf{n}''_s$—surface directors.

a monolayer where the benzene rings are coplanar with the glass plate surface (see figure 12), maximizing van der Waals adsorption forces acting between the molecules and the surface. Such a physically adsorbed layer may be mobile and therefore the molecules in it
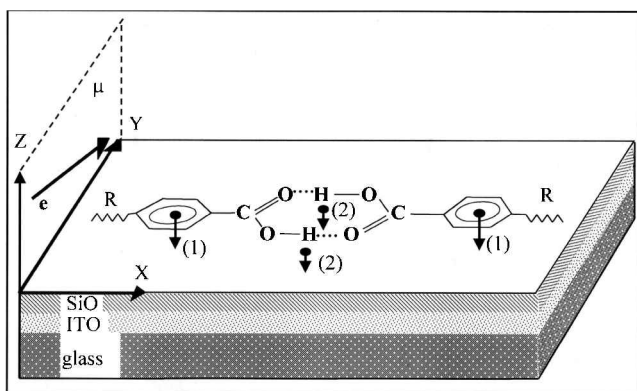

Figure 12. Schematic representation of the interaction geometry between the molecule of HOBA and the SiO/ITO/glass interface at the cell wall: (1) benzene rings, (2) hydrogen bonds in the dimer ring (the breaking of the linear hydrogen bonds creates additional bonding interaction between the molecule and the SiO/ITO surface). The dimer ring and the benzene rings are coplanar with the SiO/ITO/glass surface $x\mathrm{O}y$. In the general case $R = C_nH_{2n+1}$, where n is the homologue number; $n = 7$ for HOBA.

may arrange themselves with their axes aligned in a common direction determined by the topographic anisotropy of the SiO surface as it occurs in the bulk. For the physical–chemical mechanism it is important also that, besides the adsorption of the benzene rings—centres (1) in figure 12—by the SiO with specific energy about $10\ \mathrm{kcal\ mol^{-1}}$ [26], adsorption through hydrogen bonding exists—centres (2) in figure 12—with specific energy more than $10\ \mathrm{kcal\ mol^{-1}}$ [27]. Therefore highly anisotropic HOBA molecules, containing a few interactive parts (1) and (2) separated by the dimer ring, tend to be strongly adsorbed on a SiO surface. Such alignment on a substrate implies the presence of some kind of local anisotropic force in the vicinity of the interface liquid crystal–substrate.

The second mechanism is expressed by the anisotropic topographical structure ensuring surface elastic adaptation. This may be the most significant feature of the obliquely evaporated SiO used here, where semi-microscopic grooves or columns formed on the film surface with a spatial periodicity of a few hundred Å are believed to be responsible for the uniform monostable alignment.

Hence the induced local anisotropy due to a firmly adsorbed layer of liquid crystal molecules is present on the SiO film besides the topographical anisotropy. Thus using alignment on SiO film, we generally take into account the film topography simultaneously with the locally induced anisotropy. When both kinds of anisotropy (topographic and locally induced physical–chemical) are not correlated the actual 'easy' axis must be determined (due to competition) by the compromise reached between them. The two torque fields associated with these kinds of anisotropy participate in the surface free energy.

We suppose in turn that physical–chemical induced local anisotropy exists in the ITO/glass case as well as in the SiO/ITO/glass case and that by the bulk twist we remove only the surface torque due to the topography provided by the SiO layer.

3.3. *Theoretical analysis*

We consider the SME prevention at Ω_c as an anchoring breaking (change of the $\mathbf{n}_o$ azimuth from $\varphi \approx 0$ to $\varphi \neq 0$) leading to the smectic C layer positional transformation (which is visualized as a rotation of the long axis $\mathbf{l}$ of the SLM in figures 9, 2–5) due to domination of the bulk twist torque over the resultant (between physical–chemical and topographic) surface torque.

In a general case, calling the preferred direction for elastic adaptation due to the topography $\mathbf{n}_s$ and the

direction resulting from the physical–chemical van der Waals interaction $\mathbf{n}_v$, the surface free energy following [1, 4] can be expressed as:

$$f_s = -(1/2)W_{el}(\mathbf{n}_s \cdot \mathbf{n}_o)^2 - (1/2)W_v(\mathbf{n}_v \cdot \mathbf{n}_o)^2. \quad (1)$$

Here W_{el} and W_v are the elastic adaptation and van der Waals anchoring energy coefficients depending on the nematic–substrate interaction, $W_{el} = K_{22}/L$ and L is the extrapolation length used as a measure of the anchoring strength [25] (for $L \leqslant \xi$, where ξ is the I–N transition correlation length, the anchoring is strong). The competition between the two kinds of induced surface anisotropy, the physical–chemical and the topographic, provide a resultant 'easy' direction where the total surface energy is minimized [1, 25].

We assume that the physical–chemical local induced anisotropy is dominant in the zenithal surface energy expressed by the polar angle θ (figure 6), while in the case of a SiO obliquely evaporated layer, the more sensitive factor to the bulk twist is the azimuthal anchoring expressed more significantly by the topographic elastic adaptation [28]. Therefore in equation (1) only the first term of the surface anchoring energy f_s retained.

The balanced part of the Rapini–Papoular [4] surface energy is now:

$$f_s = (-1/2)W_{el}(\mathbf{n}_o \cdot \mathbf{n}_s)^2 = (-1/2)(K_{22}/L)\cos^2\varphi \quad (2)$$

where φ the surface azimuthal angle $= \varphi_s$, thus expressing the surface azimuthal energy (figure 6). Due to our evaporation conditions, defined by the angle of evaporation α and the thickness δ of the evaporated SiO layer, we can suppose that the zenithal energy expressed by θ is significantly higher than the azimuthal energy expressed by φ [29]. Then the φ angle will be a measure of the action and the importance of the bulk twist on the surface anchoring in our case. Using the polarization microtextural analysis for the SiO/ITO/glass case, as illustrated in figures 9, 2–5, we analyse the balance between surface torque and bulk torque. In the cases $\Omega = 0–36°$, the topographic and corresponding elastic adjustment are enough to balance the bulk torque and to keep the equilibrium between the surface and bulk forces.

Thus, when a bulk torque (Γ_b) is applied by an imposed twist on a planar oriented sample, $\mathbf{n}_s$ deviates from $\mathbf{n}_o$ giving rise to an opposite anchoring torque $\Gamma_s(\mathbf{n}_s - \mathbf{n}_o)$ or $\Gamma(\varphi)$. This can be described by a surface anchoring energy $f_s(\mathbf{n}_s - \mathbf{n}_o) = f_s(\varphi)$ minimized for $\mathbf{n}_s = \mathbf{n}_o$ as was mentioned above. An applied twist torque to the surface induces change in the φ value and provides the director $\mathbf{n}$ to follow the instantaneous torque equilibrium.

According to continuum theory [25], the free energy per unit area is obtained as the sum of the bulk elastic energy f_b and the surface anchoring f_s as follows:

$$f = f_b + f_s \quad (3)$$

where $f_s(\varphi)$ is the azimuthal component of the surface energy presented by equation (2) and f_b is the bulk elastic energy [25]. Also

$$f_b = (K_{22}/2d)(\varphi_t)^2 \quad (4)$$

where by φ_t we denote the actual twist angle which is influenced by both the bulk elastic force and the surface anchoring force of the liquid crystal. Thus φ_t will deviate from the angle Ω chosen by us and assume the angle between the 'easy' axes of the upper and lower plates. The deviation can be expressed as $\varphi = \Omega - \varphi_t$ or $\varphi_t = \Omega - \varphi$. We note that Ω is the angle between the positions of the vector $\mathbf{n}_o$ on the two plates of the cell. Thus f reads:

$$f = (K_{22}/2d)(\Omega - \varphi)^2 - (1/2)(K_{22}/L)\cos^2\varphi. \quad (5)$$

Minimizing (5), i.e. solving $\delta f/\delta \varphi = 0$, and neglecting the higher order of $\Omega(\Omega^2)$ we obtain the torque balance equation (the torque equilibrium):

$$(2K_{22}/d)(\Omega - \varphi) - (K_{22}/L)\sin 2\varphi = 0. \quad (6)$$

From this equation the surface anchoring strength $W_{el} = K_{22}/L$ is expressed as:

$$W_{el} = 2K_{22}(\Omega - \varphi)/(d\sin 2\varphi) \quad (7)$$

or

$$1/L = 2(\Omega - \varphi)/(d\sin 2\varphi). \quad (8)$$

Consequently, from equations (7) and (8) it follows that when φ approaches Ω, W_{el} tends to zero and, respectively, L tends to infinity and on the contrary, when φ tends to zero (diminution of the twist), L tends to zero. This behaviour of the parameter L expresses anchoring breaking or surface instability observed as SME prevention.

Expressing the phenomenon described in terms of the SmC texture, this means a transition from a texture where the SLM long axes $\mathbf{l}$ are oriented along the directions $\pm\pi/4$ (for $0 < \Omega < 36°$, figure 10) to a texture where these monodomains are oriented with $\mathbf{l} \perp \mathbf{n}_o$ or $\mathbf{l} \parallel \mathbf{n}_o$ (for $70° < \Omega < \pi/2$, see figure 11, which we consider as disorder with respect to the case $(\mathbf{l}^\wedge \mathbf{n}_o) = \pm\pi/4$) and this is not memorized in the nematic phase since the bulk twist prevents the surface memorization, inducing a surface anchoring instability.

Finally, with the experiments presented now, we could only deduce approximate information about the value of the component $\delta\mathbf{Q}$ ($\approx 0.4\,eV$ in our case, obtained as the difference between Q measured for SiO/ITO/glass and ITO/glass coatings—see §2) of the erasure activation

energy Q. We assume that δQ is due to a pure elastic adaptation at the grooved surface imposed by SiO evaporation. For a more exact calculation of δQ we must use a regular holographic grating, where the relief profile is regular and the Berreman model [5] enables calculation of the theoretical pure elastic anchoring. Last but not least, we assume that bulk twist depresses double electric layer formation which is a decisive component for stronger surface memorization in the case of a conducting surface (such as SiO/ITO/glass), as considered here [7, 30].

4. Conclusions

Imposing a mechanical counteraction provided by a bulk twist, we succeeded in preventing the surface memorization of smectic C textures in the temperature range of the nematic phase of 4-*n*-heptyloxybenzoic acid oriented by an obliquely evaporated SiO layer. In order to avoid the erasure action of the thermal energy $k_B T$, we kept the temperature of the nematic phase constant. Assuming that for strong anchoring provided by the SiO evaporation parameters the angle between the 'easy' directions of the upper and the lower orienting plates is approximately equal to the real bulk twist angle, we found a twist angle $\Omega_c = 70°$ where the surface memorization is prevented in the region $71° < \Omega < \pi/2$. Using the same substance, twist and temperature in the N phase of HOBA, but changing the surface conditions—the cell walls are covered only with ITO—we found that there is no bulk twist in the entire interval $0° < \Omega < \pi/2$ which is able to prevent the surface memorization.

A qualitative explanation of the phenomenon is suggested. We assume that the anisotropy of the surface necessary for the anchoring and orientation is provided by two components: (a) one induced by the anisotropic part of the van der Waals forces of interaction between the orienting surface and the first liquid crystal monolayer (locally induced anisotropy); (b) a topographical part due to the SiO evaporation providing elastic adaptation of the liquid crystal molecules on the surface. Since on the ITO surface the memorization always exists, we assume that the memorization prevention in the SiO case is due to the disturbance of the balance between the bulk and the surface torques during the increase of the bulk twist imposed by us. We accept that the resultant anisotropy (from the two surface torques—the locally induced anisotropy and the topographical elastic anisotropy) necessary to maintain the molecular 'easy' directions decreases with the increasing bulk twist by the value equal to the topographical anisotropy provided by the SiO evaporation.

We found that a sufficiently high value of the $\mathbf{n}_s$ azimuthal deviation (φ) with increasing Ω provides values of the anchoring strength parameters $W_{el} \to 0$ and $L \to \infty$

which means an anchoring breaking (surface instability) preventing surface memorization. Thus this surface instability due to the loss of topographical anisotropy provided by the SiO layer changes the surface conditions for growth of the vertical (in our case) smectic layers indicated by their SLMs with a $\pm\pi/4$ angle with respect to the initial orientation corresponding to $\mathbf{n}_o$. By micro-textural polarization analysis we found that the long axis (meaning the layer plane direction $\mathbf{s}$) changes its position due to the imposed bulk twist from the angle range $\pm\pi/4$ with the 'easy' direction $\mathbf{n}_o$ to one including the angle 0 or $\pm\pi/2$ with this direction. Obviously such surface instability does not favour the surface memorization. By a qualitative analysis of the actions of the resultant surface and bulk torques, we found the conditions expressed by the value of the surface extrapolation length for the surface anchoring transition. We also estimated the contribution of the term δQ to the erasure activation energy Q of the surface memorization.

References

[1] YOKOYAMA, H., KOBAYASHI, S., and KAMEI, H., 1984, *J. appl. Phys.*, **56**, 2645.
[2] CLARK, N. A., 1985, *Phys. Rev. Lett.*, **55**, 292.
[3] PETROV, M., and TSONEV, L., 1996, *Liq. Cryst.*, **21**, 543.
[4] RAPINI, A., and PAPOULAR, M., 1969, *J. Phys. (Fr.)*, **30**, Col. 4, C4-C5.
[5] BERREMAN, D. W., 1973, *Mol. Cryst. liq. Cryst.*, **23**, 215.
[6] TSONEV, L., PETROV, M., and BARBERO, G., 1998, *Liq. Cryst.*, **24**, 853.
[7] TSONEV, L., PETROV, M., and BARBERO, G., 2000, *Liq. Cryst.*, **27**, 825.
[8] TSONEV, L., and PETROV, M., 2000, *Liq. Cryst.*, **27**, 1691.
[9] OUCHI, Y., FELLER, M. B., MOSES, T., and SHEN, Y. R., 1992, *Phys. Rev. Lett.*, **68**, 3040.
[10] JEROME, B., 1991, *Rep. Prog. Phys.*, **54**, 391.
[11] PETROV, M., and SIMOVA, P., 1985, *J. Phys. D*, **18**, 239.
[12] FRUNZA, S., FRUNZA, L., PETROV, M., SPARAVIGNA, A., and TORGOVA, S., 1996, *Mol. Mater.*, **6**, 215.
[13] PETROV, M., ANACHKOVA, E., KOROV, N., RATAJCZAK, H., and BARAN, J., 1994, *J. mol. Liq.*, **62**, 221.
[14] BARBERO, G., KOMITOV, L., PETROV, M., and STRIGAZZI, A., 1993, *Int. J. mod. Phys.*, **B5**, 2229.
[15] NEUBERT, M. F., and DE VRIES, A., 1987, *Mol. Cryst. liq. Cryst.*, **145**, 1.
[16] PETROV, M., BRASLAU, A., LEVELUT, A. M., and DURAND, G., 1992, *J. Phys. II (Fr.)*, **2**, 1159.
[17] PETROV, M., and DURAND, G., 1996, *J. Phys. II (Fr.)*, **6**, 1259.
[18] DE VRIES, A., 1967, *Mol. Cryst. liq. Cryst.*, **10**, 555.
[19] FRUNZA, S., FRUNZA, L., PETROV, M., and BARBERO, G., 1998, *Liq. Cryst.*, **2**, 215.
[20] MONKADE, M., BOIX, M., and DURAND, G., 1988, *Europhys. Lett.*, **5**, 697.
[21] JEROME, B., PIERANSKI, P., and BOIX, M., 1988, *Europhys. Lett.*, **5**, 693.
[22] NEIUWENHIUZEN, J. M., and HAANSTRA, H. B., 1966, *Philips tech. Rev.*, **3**, 87.

[23] HENDERSEN, D., BRODSKY, M. H., and CHANDHARI, P.,
     1974, *Appl. Phys. Lett*., **25,** 641.
[24] VAN SPRANG, H. A., and AARTSEN, R. G., 1984, *J. appl.
     Phys*., **56,** 251.
[25] DE GENNES, P. G., and PROST, J., 1993, *The Physics of
     Liquid Crystals* (Oxford: Clarendon Press).
[26] YOKOYAMA, H., KOBAYASHI, S., and KAMEI, H., 1983,
     Mol. Cryst. liq. Cryst., **99,** 39.

[27] DELOCHE, B., and CABANE, B., 1971, *Mol. Cryst. liq.
     Cryst*., **19,** 25.
[28] NOBILI, M., BARBERI, R., and DURAND, G., 1995, *J. Phys.
     II (Fr.)*, **5,** 531.
[29] SERGAN, V., and DURAND, G., 1995, *Liq. Cryst*., **18,** 171.
[30] BARBERO, G., and DURAND, G., 1990, *J. appl. Phys*., **67,**
     2678; BARBERO, G., and DURAND, G., 1990, *J. Phys.
     (Fr.)*, **51,** 281.